PEDIATRICS INTERNATIONAL Official Journal of the Japan Pediatric Society

Pediatrics International (2020) **62**, 347–356 doi: 10.1111/ped.14108

Original Article

Developing a newborn rat model of ventriculitis without concomitant bacteremia by intraventricular injection of K1 (−) *Escherichia coli*

So Yoon Ahn,[1†] Yun Sil Chang,[1,2†] Dong Kyung Sung,[1] Young Eun Kim[2] and Won Soon Park[1,2]

[1]*Department of Pediatrics, Samsung Medical Center and* [2]*Samsung Biomedical Research Institute, Sungkyunkwan University School of Medicine, Seoul, Korea*

Abstract ***Background*:** Neonatal meningitis caused by *Escherichia coli* results in high mortality and neurological disabilities, and the concomitant systemic bacteremia confounds its mortality and brain injury. This study developed an experimental model of neonatal ventriculitis without concomitant systemic bacteremia by determining the bacterial inoculum of K1 capsule-negative *E. coli* by intraventricular injection in newborn rats.

***Methods*:** We carried out intraventricular injections 1×10^2 (low dose), 5×10^2 (medium dose), or 1×10^3 (high dose) colony-forming units (CFU) of K1 (−) *E. coli* (EC5ME) in Sprague-Dawley rats at postnatal day (P) 11. Ampicillin was started at P12. Blood and cerebrospinal fluid (CSF) cultures were performed at 6 h, 1 day, and 6 days after inoculation. Brain magnetic resonance imaging (MRI) was performed at P12 and P17. Survival was monitored, and brain tissue was obtained for histological and biochemical analyses at P12 and P17.

***Results*:** Survival was inoculum dose-dependent, with the lowest survival in the high-dose group (20%) compared with the medium- (67%) or low- (73%) dose groups. CSF bacterial counts in the low- and medium-dose groups were significantly lower than that in the high-dose group at 6 h, but not at 24 h after inoculation. No bacteria were isolated from the blood throughout the experiment or from the CSF at P17. Brain MRI showed an inoculum dose-dependent increase in the extent of brain injury and inflammatory responses.

***Conclusions*:** We developed a newborn rat model of bacterial ventriculitis without concomitant systemic bacteremia by intraventricular injection of EC5ME.

Key words infant, meningitis, newborn, stem cells.

Despite continuous improvements in antibiotic therapy and intensive care medicine, bacterial meningitis remains a serious disease at any age, and the prognosis is particularly poor in newborn infants, with mortality rates of 20–40% and long-term neurological sequelae, including deafness, blindness, seizures, hydrocephalus, and cognitive impairment in up to 50% of survivors.[1–3] The precise mechanisms by which bacterial infection and the ensuing inflammatory responses in the subarachnoid space during neonatal bacterial meningitis lead to neuronal injury, which could result in death or neurological sequelae in survivors, are not completely delineated. Therefore, a better understanding of the mechanism of brain damage is necessary to prevent this neuronal injury and, consequently, to reduce the mortality and morbidities associated with neonatal bacterial meningitis.

Correspondence: Won Soon Park, MD PhD, Department of Pediatrics, Samsung Medical Center, Sungkyunkwan University School of Medicine, 81, Irwon-ro, Gangnam-gu, Seoul, South Korea, 06351. Email: wonspark@skku.edu; ws123.park@samsung.com

[†]Co-first authors.

Received 27 April 2019; revised 11 December 2019; accepted 13 December 2019.

Developing an appropriate animal model that could simulate clinical bacterial meningitis in newborn infants is essential to determine its pathogenesis and to test the efficacy of newly developed adjuvant treatments, in addition to the use of antibiotics. Currently, several animal models of neonatal bacterial meningitis, including newborn piglets,[4] mice,[5–7] rats,[8,9] and rabbits[10] are available, and meningitis was induced by various routes, including intraperitoneal,[5,11] intranasal,[6] intravenous,[5,10,12] and intracisternal[7–10,12] inoculation of bacteria. However, these animal models have certain drawbacks, including small sample size, low infectivity, high mortality, and/or variable extent of brain injury.[11] Furthermore, concomitant bacteremia might aggravate the meningitis-induced brain injury,[9,13,14] thus increasing mortality.[8,9,15] Therefore, in the present study, we developed a newborn rat model of neonatal bacterial ventriculitis to mimic the human clinical and neuropathological meningitis, using 11-day-old newborn Sprague–Dawley rats, with titrated intraventricular inoculation of *Escherichia coli*, (*E. coli*) the most common gram-negative pathogen of neonatal bacterial meningitis.[3] We attempted to determine the bacterial inoculum dose with maximal brain injury and minimal mortality by using K1 capsule-negative *E. coli* to confine the infection to the central nervous system,

without concomitant systemic bacteremia.[12,16] We inoculated the bacteria intraventricularly using a stereotaxic frame to simulate the neuropathological progression of clinical neonatal bacterial meningitis, which begins with ventriculitis.[17,18] Brain injury was monitored *in vivo* by brain magnetic resonance imaging (MRI).[19–22]

Methods

Infecting organism

In this study we used EC5ME, an un-encapsulated mutant of *E. coli* strain possessing the K1 capsular polysaccharide C5 (serotype 018:K1:H7) (a kind gift from Professor Kwang Sik Kim, Johns Hopkins University, MD, USA)[12,16] to induce only bacterial ventriculitis. Bacteria were cultured overnight in brain-heart infusion broth, diluted in fresh medium, and grown for another 6 h to the mid-logarithmic phase. The culture was centrifuged at 5,000 × *g* for 10 min, re-suspended in sterile normal saline to the desired concentration, and used for the intraventricular injection. The accuracy of the inoculum size was confirmed by serial dilution, overnight culture on blood agar plates, followed by a count of colony-forming units (CFU).

The experimental protocols described herein were reviewed and approved by the Animal Care and Use Committee of Samsung Biomedical Research Institute, Seoul, Korea. This study was also performed in accordance with Institutional and National Institutes of Health Guidelines for Laboratory Animal Care.

Animal model of ventriculitis

Figure 1 shows details of the experimental schedule. The experiment began at postnatal day (P) 11 and continued to P17. To induce ventriculitis, newborn Sprague–Dawley rats (Orient Co, Seoul, Korea) were anesthetized using 2% isoflurane in oxygen-enriched air and a total of 10 μL EC5ME inoculum in saline was slowly infused into the left ventricle under stereotactic guidance (Digital Stereotaxic Instrument with Fine Drive, MyNeurolab, St. Louis, MO, USA) coordinates: $x = \pm 0.5$, $y = \pm 1.0$, $z = \pm 2.5$ mm relative to the bregma) at P11. To determine the optimal inoculum dose with minimal mortality and maximal brain injury, we tested three different inoculum doses of *E. coli*: a low inoculum (LE) dose of 1×10^2 CFU EC5ME, a medium inoculum (ME) dose of 5×10^2 CFU EC5ME, and a high inoculum (HE) dose of 1×10^3 CFU EC5ME. For the normal control group (NC), an equal volume of normal saline was given intraventricularly. After the procedure, the rat pups were allowed to recover and returned to their dams; there was no mortality associated with the procedure.

Ten rat pups for each group were allocated to assess the acute pathophysiological changes, and the survivors were sacrificed at 24 h (P12) after bacterial inoculation for histopathological assessment (n = 6, 5, 4, and 3 for the NC, LE, ME, and HE groups, respectively) and biochemical analyses (n = 4, 4, 4, and 3 for the NC, LE, ME, and HE groups, respectively). Using these short-term groups, cerebrospinal fluid (CSF) was obtained using a cisternal tap to determine the bacterial titer at 6 and 24 h after bacterial injection. We also conducted a time course experiment in 10 animals for each group, to determine the survival rate until sacrifice of the survivors at P17 for histopathological assessment (n = 5, 4, 4, and 2 for the NC, LE, ME, and HE groups, respectively) and biochemical analyses (n = 5, 3, 4, and 0 for the NC, LE, ME, and HE groups, respectively). Intraperitoneal injection of ampicillin (200 mg/kg/day) was started 6 h after bacterial inoculation and continued for 3 days until P13. With these long-term groups, CSF was also drawn before sacrifice at 6 days after ventriculitis induction (P17).

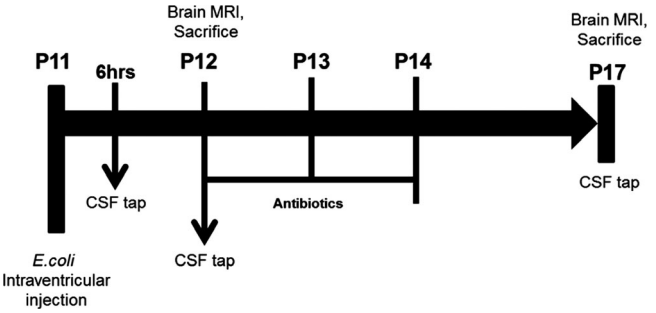

Fig. 1 Experimental protocol. *E. coli* was injected intra-cerebroventricularly on postnatal day (P) 11 at different doses for each group: low dose 1×10^2 colony-forming units (CFU), medium dose 5×10^2 CFU, and high dose 1×10^3 CFU. Brain magnetic resonance imaging was performed before the rats were sacrificed. CSF, cerebrospinal fluid.

Intraperitoneal injection of ampicillin (200 mg/kg/day) was started 24 h after bacterial inoculation and continued for 3 days. Brain MRI was performed at P12 and P17. The body weight of all rats was measured daily and was sacrificed at P12 and P17 under deep pentobarbital anesthesia (60 mg/kg, intraperitoneal). Immediately after extracting the brain, fresh brains were weighed. To assess the possible side effects of the injection, brain histology at P17 was assessed after needle injection into the ventricles only at P11 (Appendix S1).

Bacterial quantification

Bacterial concentrations from each study group were measured in the CSF and blood at 6 h, 24 h, and 6 days after bacterial inoculation for induction of ventriculitis. Bacteria CFU levels in the CSF and blood were measured at dilutions of 10^{-4}–10^{-8} plated on brain heart infusion agar after overnight incubation at 37°C.

In vivo brain MRI assessment

Brain MRI was performed while the rats were kept in an anesthetized state by the administration of 1.5–2% isoflurane in

oxygen-enriched air using a facemask. All MRI was performed using a 7.0-tesla MRI System (Bruker-Biospin, Fällanden, Switzerland) prepared with a 20 cm gradient set capable of providing a rising time of 400 mTm-1. The MR images were acquired with 1.0-mm slice thickness, and a total of 12 slices were acquired. Brain MRI was performed at P12 (n = 10, 9, 8, and 6 in the NC, LE, ME, and HE groups, respectively) and at P17 (n = 11, 7, 8, and 2 in the NC, LE, ME, and HE groups, respectively). After MRI , the rat pups were allowed to recover and were returned to their dams.

Measurement of the extent of brain injury by MRI

All MR images were analyzed using Image J software (National Institutes of Health). The infarcted lesion was well identified by the hyperintense areas in T2-weighted imaging at P12 and P17. The area of infarcted hyperintense cortical lesion, lateral ventricles, and whole brain were measured in serial brain MRI sections and the areas were summed to calculate volume. The ratio of the infarcted regional volume to the whole brain volume was calculated as a parameter of brain injury, injury area volume ratio. The ratio of the ventricle volume to the whole brain volume was also calculated as the ventriculomegaly volume ratio.

Tissue preparation

Brain tissue preparation procedures were performed in the surviving rats until P12 (n = 10, 9, 8, and 6 in the NC, LE, ME, and HE groups, respectively) and P17 (n = 10, 7, 8, and 2 in the NC, LE, ME, and HE groups, respectively). The animals were anesthetized with sodium pentobarbital (100 mg/kg), and their brains were isolated after thoracotomy and transcardiac perfusion with ice-cold 4% paraformaldehyde in 0.1 mol/L phosphate-buffered saline. The brains were carefully removed from the animals and fixed overnight with 4% formaldehyde solution at room temperature. The brains were embedded in paraffin and coronal serial sections (4-μm thick) were taken from the paraffin blocks for morphometric analyses at the level of the medial septum area (+0.95 mm to −0.11/bregma) and the hippocampal area (−2.85 to − 3.70 mm). The sections were stained with hematoxylin and eosin to assess the extent of neuronal damage.

TUNEL assay

Cell death in the hippocampal region was assessed using the immunofluorescent terminal deoxynucleotidyl transferase-mediated deoxyuridine triphosphate nick-end labeling (TUNEL) technique (kit G3250, Promega, Madison, WI, USA). The slides were mounted with Vectashield mounting solution with 4′, 6′-diamidino-2-phenylindole dihydrochloride hydrate (DAPI; H-1200; Vector) and visualized by 20× (dentate gyrus) and 5× tile-scan confocal microscopy (Leica, Wetzlar, Germany). A blinded evaluator counted the density of TUNEL-positive nuclei in whole brain on coronal brain sections. Six coronal sections (+0.95 mm to −0.11 mm/bregma) were counted from each brain.

Immunohistochemistry

Immunohistochemistry of gliosis (neuronal-specific glial fibrillary acidic protein [GFAP]) and reactive microglia (ED-1) was performed on deparaffinized 4-μm thick brain sections. The slices were incubated with the primary anti-GFAP antibodies (rabbit polyclonal; Dako, Glostrup, Denmark), overnight, 4°C, 1:1,000 in phosphate-buffered saline (PBS) with 1% bovine serum albumin and the anti-ED-1 antibodies (mouse polyclonal; (Millipore, CA, USA), overnight, 4°C, 1:500 in PBS with 1% bovine serum albumin. After three rinses (same buffer), each section was incubated with Alexa Fluor 568 (red) conjugated anti-rabbit immunoglobulin 90 min, diluted 1:50; (Molecular Probes, Eugene, OR, USA) and Alexa Fluor 568 (red) conjugated anti-mouse immunoglobulin 90 min, diluted 1:500 (Molecular Probes). After three rinses, the sections were mounted with Vectashield mounting solution containing 4′, 6′-diamidino-2-phenylindole dihydrochloride hydrate and visualized by 20× (dentate gyrus) and 5× tile-scan confocal microscopy (Leica). The density of GFAP-positive cells and the number of ED-1-positive cells were determined by a blinded observer in whole tile-scan fields of each animal's brain, using ImageJ software.

Enzyme-linked immunosorbent assay (ELISA)

IL-1α, IL-1β, IL-6, and TNF-α concentrations in tissue homogenates were measured at P12 and P17 using the Milliplex MAP ELISA Kit (Millipore, Billerica, MA, USA) according to the manufacturer's protocol.

Statistical analyses

Statistical analyses were performed using SPSS, version 18.0 (IBM Corp., Armonk, NY, USA). Data are expressed as the mean ± standard error of the mean. For continuous variables, statistical comparison between groups was performed using one-way analysis of variance (ANOVA) and Tukey's post hoc analysis. $P < 0.05$ was considered statistically significant

Results

Survival rates and weight

Figure 1 shows the details of the experimental schedule. The experiment began at P11 and continued through to P17. To induce ventriculitis, at P11, three different doses of *E. coli* were injected into the cerebroventricles of newborn rats; LE dose of 1×10^2 CFU EC5ME, an ME dose of 5×10^2 CFU EC5ME, and an HE dose of 1×10^3 CFU EC5ME . The survival rate after induction of bacterial ventriculitis was bacterial inoculum dose-dependent, showing the lowest survival rate up to P17 of 20% for the HE dose and 67% and 73% for the ME and LE

doses, respectively (Fig. 2a). While the survival rate up to P17 in the HE group was significantly lower compared to that in the NC group, the survival rate of the LE and ME groups was not significantly reduced compared with the NC group.

While birth body and brain weight in each study group was not significantly different between the study groups; the body weight gain at P17 in the LE, ME, and HE groups was significantly lower, the brain weight gain in the ME and HE groups was significantly lower, and the brain/body weight ratio in the ME and HE groups was significantly higher compared with the those in the NC group. The least body and brain weight gain, and the highest brain/body ratio, were observed in the HE group compared with those in the LE and ME groups (Fig. 2b–d).

Bacterial counts

At 6 h (P11) and 24 h (P12) after bacterial injection, to evaluate the bacterial burdens, the CFU were counted in the CSF and blood from each study group before sacrifice. Also, at 6 days after induction of ventriculitis (P17), CSF was drawn from each study group before sacrifice. While no bacterial growth in the blood was detected in all study groups throughout the experiment, the bacterial counts in the CSF at 6 h after the induction of ventriculitis in both the LE and ME were significantly lower compared with that in the HE group. Thereafter, the bacterial counts in the CSF of all study groups increased significantly compared with that at 6 h, and there were no significant inter-group differences at 24 h after the induction of ventriculitis (Fig. 3). No bacterial growth in the CSF was detected in any of the study groups at 6 days after the induction of ventriculitis.

Brain MRI

To assess the extent of ventriculitis-induced brain infarction and hydrocephalus, *in vivo* brain MRI was performed. The degree of the brain infarct in the ipsilateral cortex and the dilatation of the ventricle to whole brain, as evidenced by the hyperintense areas in the diffusion-weighted MRI, performed at P12 and by T2-weighted MRI, performed at P17 were measured.

The brain infarct volume ratios at P12 and P17 were bacterial inoculum dose-dependently increased, showing the highest ratio in the HE group, and a seemingly increased ratio in the

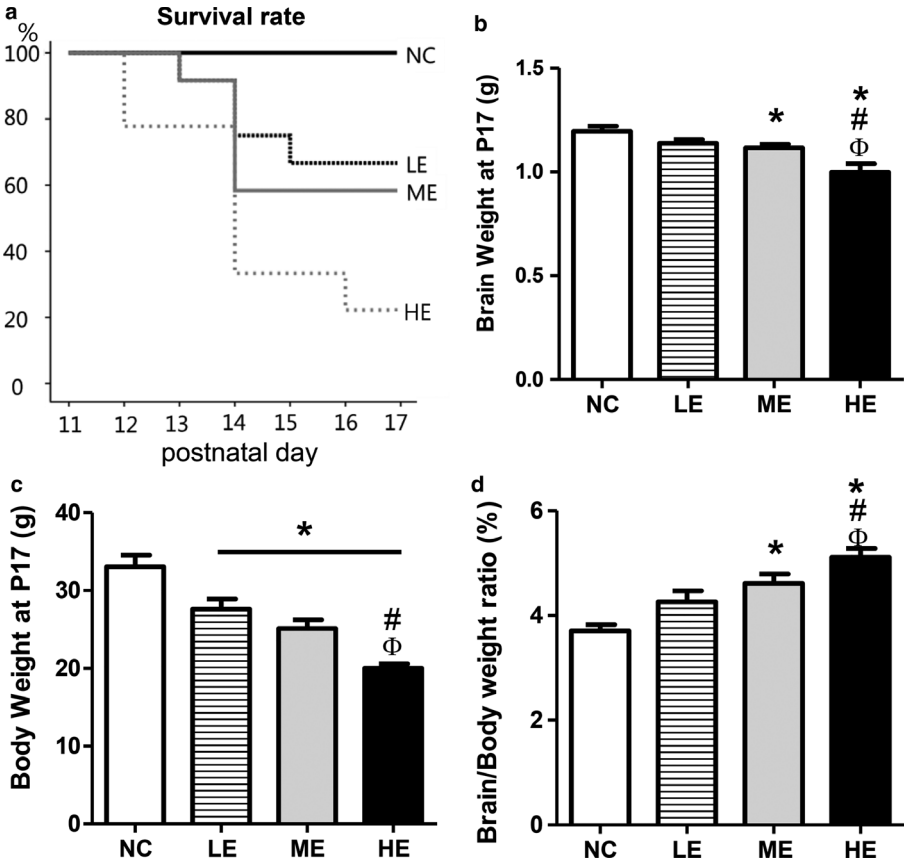

Fig. 2 Survival rates. (A) Survival rates in each group were determined using Kaplan–Meier analysis followed by a log-rank test group. (B) Brain weight and (C) body weight were measured at postnatal day (P)17 in each group (n = 11, 7, 9, and 2 in the normal control (NC), low-dose (LE), medium-dose (ME), and high-dose (HE), respectively). Both weights decreased significantly depending on the *E. coli* dose. (D) The ratio of brain weight: body weight significantly increased in the HE group compared with the other groups. Data are presented as the mean ± standard error of the mean (SEM). $^{*}P < 0.05$ compared with the normal control (NC) group, $^{\#}P < 0.05$ compared with the LE group, $^{\$}P < 0.05$ compared with the ME group.

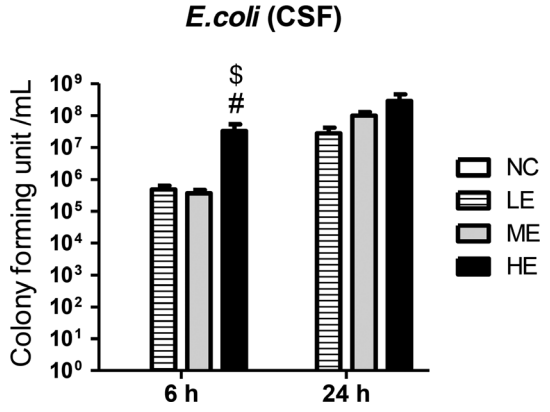

Fig. 3 Bacterial counts in the cerebrospinal fluid (CSF). Bacterial counts in the CSF obtained at 6 and 24 h after bacterial inoculation and before initiation of antibiotic treatment. Data are presented as the mean ± SEM. *E. coli* groups: $^{\#}P < 0.05$ compared to the LE group, $^{\$}P < 0.05$ compared to the ME group NC, normal control; LE, low-dose; ME, medium-dose; HE, high-dose (*E. coli* groups); h, hour.

ME group compared with that in the LE group that did not reach statistical significance (Fig. 4). The ventriculomegaly volume ratios at P12 were bacterial inoculum dose-dependently increased, showing the highest increase in the HE group compared with the LE and ME groups. In addition, although the absolute extent of ventriculomegaly was significantly reduced compared with P12, the ventriculomegaly volume ratios at P17 were also bacterial inoculum dose-dependently increased, showing the highest increase in the HE group compared with the LE and ME groups (Fig. 4).

TUNEL staining and immunohistochemistry

To assess the extent of bacterial ventriculitis-induced cell death, reactivate gliosis, and microglia in the brain, the number of TUNEL- and ED-1 (Ectodysplasin A)-positive cells, and the density of GFAP-positive cells in the hippocampus were estimated at 24 h after induction of ventriculitis (P12). The number of TUNEL- and ED-1-positive cells, and the intensity of GFAP-positive cells in the hippocampus at P12 were bacterial inoculum dose-dependently increased compared with the NC group, showing the highest increase in the HE group. The increased number of TUNEL-positive cells and the intensity of GFAP-positive cells in the ME group were significantly higher compared with those in the LE group (Fig. 5).

Inflammatory cytokines in brain

Levels of inflammatory cytokines, such as interleukin (IL)-1α, IL-1β, IL-6, and tumor necrosis factor alpha (TNF-α), measured in the periventricular brain tissue homogenates at P12 revealed a bacterial inoculum dose-dependent increase, showing the highest increase in the HE group. The inflammatory cytokine levels in the ME group were significantly higher compared with those in the LE group (Fig. 6). Although the brain homogenates of the HE group were not available for measurement because of their high mortality at P17, and the absolute levels of the inflammatory cytokines were significantly reduced compared with P12, the inflammatory cytokines were bacterial inoculum dose-dependently increased, showing significantly higher levels in the ME group compared with those in the LE group.

Discussion

Despite recent improvements in neonatal intensive care medicine and the development of highly active new antibiotics, neonatal bacterial meningitis remains a serious disease with high mortality and neurological morbidities in survivors.[1,3] Currently, few effective adjuvant therapies are available to improve the prognosis of this intractable and devastating neonatal disorder. Therefore, developing an appropriate animal model to simulate clinical bacterial meningitis in newborn infants is an essential first step to determining its pathophysiological mechanisms, and to test the therapeutic efficacy of any potential new treatments. However, the limitations of currently available experimental models of meningitis lie in the wide variability among the species, the inoculation methods, and the age of the animal models.[11]

In this study, we used P11 rats as an animal model of neonatal ventriculitis because the rat brain at P11 is comparable in terms of maturation to the human brain at birth.[23] The large litter size provides a considerable number of rat pups per experimental induction of meningitis setup. Also, the larger size of rat pups compared with mice enables easier surgical manipulation at an earlier age and a larger amount of brain tissues obtained at harvest. Furthermore, with our already established newborn rat model of severe intraventricular hemorrhage (IVH),[20–22] middle cerebral arterial occlusion,[24] and hypoxic-ischemic encephalopathy[25] with *in vivo* brain MRI and histopathological analyses, the pathophysiological mechanisms and therapeutic efficacy could be easily extrapolated to develop a newborn rat model of ventriculitis in this study. To inject bacteria into the brain ventricles, the identical injection technique using stereotaxic guidance that we used in our previous study, induced severe IVH by intraventricular injection of blood in the much younger newborn rat at P4[20] than the newborn rat at P11 used in this study. Overall, the findings of the present study suggested that the newborn rat pup model is suitable and appropriate to research the pathogenesis of neonatal bacterial ventriculitis and to test the efficacy of new treatments.

In a clinical setting, newborn meningitis usually develops with concomitant sepsis. The concomitant bacteremia with meningitis in the newborn rat pup animal model is associated with high mortality and, thus, it was hard to generate and evaluate meningitis-induced brain injury in live rats. In addition, though brain damage was primarily caused by local meningeal infection, accompanying sepsis might exacerbate the severity of brain injury and mortality.

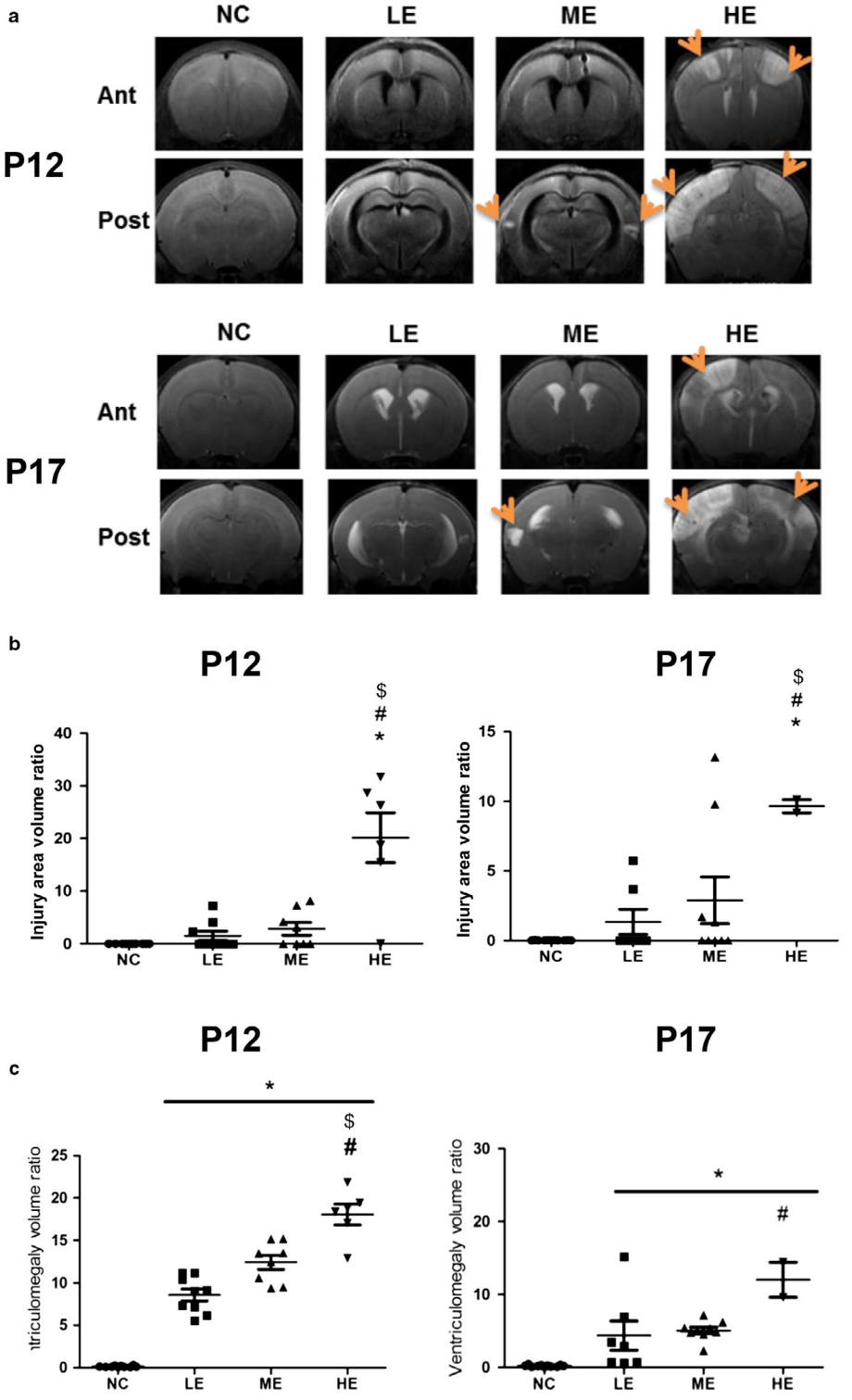

Fig. 4 Evolution of brain injury at postnatal day (P)12 and P17. (a) Representative brain magnetic resonance imaging (MRI) of the normal control (NC) (no *E. coli* control) (left column), low-dose (LE) *E. coli* group (middle left column), medium-dose (ME) *E. coli* group (middle right column), and high-dose (HE) *E. coli* group (right column) groups from the medial septal area on day 1 and day 6 after meningitis (P12 and P17). (b) The intact volume of the cortex area-to-whole brain ratio and (c) the ventriculomegaly volume ratio were measured by MRI at P12 and P17. Data are presented as the mean ± SEM. $^{*}P < 0.05$ compared with the NC group, $^{\#}P < 0.05$ compared with the LE group, $^{\$}P < 0.05$ compared with the ME group.

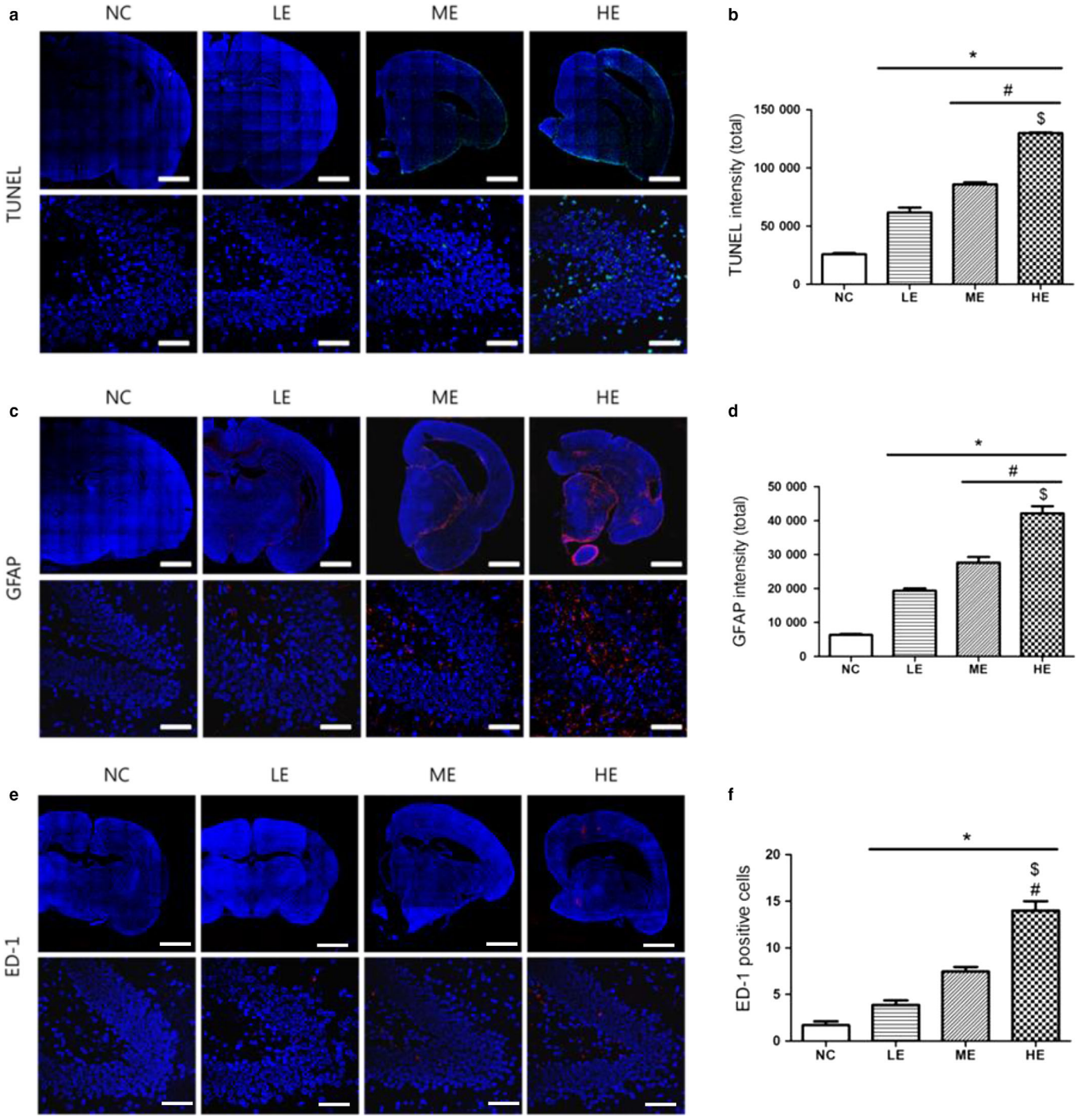

Fig. 5 Immunostaining in the hippocampus region. Representative photomicrographs of (A) terminal deoxynucleotidyl transferase-mediated deoxyuridine triphosphate nick-end labeling (TUNEL), (C) glial fibrillary acidic protein (GFAP) intensity, and (E) reactive microglia (ED-1)-positive cells in the brain hippocampus of postnatal day (P)12 rats at low magnification (upper panel) and high magnification (lower panel) in each group. TUNEL intensity was labeled with fluorescein isothiocyanate (FITC; green); GFAP and ED-1-positive cells were labeled with tetramethylrhodamine isothiocynate (TRITC; red). The cell nuclei were labeled with 4′,6-diamidino- 2-phenylindole (DAPI; blue) (Scale bar = 25 μm). The average intensity of observed (B) TUNEL and (D) GFAP, and the average number of (F) ED-1-positive cells per high-power field in each group are also represented. Data are presented as the mean ± SEM. $^{*}P < 0.05$ compared with the normal control (NC) group, $^{\#}P < 0.05$ compared with the LE group, $^{\$}P < 0.05$ compared with the ME group. LE, low-dose; ME, medium-dose; HE, high-dose (*E. coli* groups).

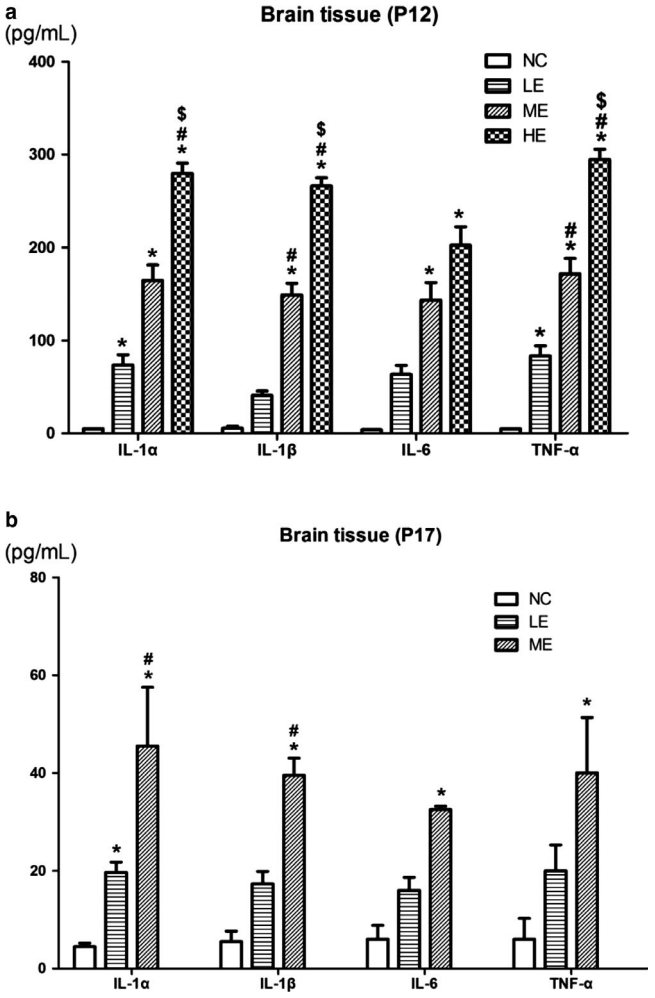

Fig. 6 Inflammatory cytokines of brain. Interleukin [IL]-1α, IL-1β, IL-6, and tumor necrosis factor [TNF]-α concentrations in brain tissue homogenates at (A) postnatal day (P) P12 and (B) P17, were measured using enzyme-linked immunosorbent assay (ELISA) in each group. Data are presented as the mean ± SEM. $^{*}P < 0.05$ compared with the NC group, $^{\#}P < 0.05$ compared with the LE group, $^{\$}P < 0.05$ compared with the ME group. LE, low-dose; ME, medium-dose; HE, high-dose (*E. coli* groups).

To reduce the meningitis-induced sequelae and to improve outcome and survival, we aimed to make a theoretical model that can dissect meningitis injury from systemic septic shock and, thus, make it possible to assess and monitor the degree of meningitis-induced brain damage.

The presence of K1 capsule and a high degree of bacterial concentration (>104 CFU/mL), but not the collapse of the blood-brain barrier (BBB), are two key determinants for the development of *E. coli* meningitis and secondary bacteremia. Thus, our data of no concomitant K1 capsule-negative *E. coli* secondary bacteremia, despite their high bacterial concentrations in the CSF also confirms the critical role of K1 capsule without impairment of BBB for inducing *E. coli* bacterial ventriculitis and secondary bacteremia. In the present study, by using K1 capsule-negative *E. coli* we could induce neonatal bacterial ventriculitis in the new rat pup model and prevented the confounding aggravation of mortality and brain injury by concomitant bacteremia.

The neuropathology of neonatal bacterial meningitis begins with choroid plexitis and ventriculitis [18,26,27] and progresses to arachnoiditis and vasculitis, leading to brain edema, hydrocephalus, infarction, and periventricular leukomalacia.[28] In the present study, *K1 (−) E. coli* was injected intraventricularly to induce ventriculitis and it bypasses the natural hematogenous bacterial invasion across the BBB into the CNS. This model appears to be similar to the condition of ventriculitis that typically happens to ventriculo-peritoneal shunt patients with shunt infection. Furthermore, the neuropathology of neonatal bacterial meningitis begins with choroid plexitis and ventriculitis[17,18,27] and progresses to arachnoiditis and vasculitis, leading to brain edema, hydrocephalus, infarction, and periventricular leukomalacia.[28] In the present study, K1 (−) *E. coli* was injected intraventricularly to induce ventriculitis. Although it bypasses the natural hematogenous bacterial invasion across the BBB into the CNS, it might first cause ventriculitis, which simulates neonatal bacterial meningitis in the clinical setting.

In the present study, we tested three different doses of K1 (−) *E. coli* for the induction of ventriculitis to determine the optimal inoculum dose with minimal mortality and maximal brain injury; 1×10^2 CFU for the LE group, 5×10^2 CFU for the ME group, and 1×10^3 CFUs for the HE group. Survival rates, body and brain weight gain, the extent of inflammatory responses, and brain injury correlated significantly with the inoculum dose used to induce ventriculitis, showing highest mortality, extent of inflammatory responses, and brain injury, and the least body and brain weight gain in the HE group. We also observed higher inflammatory responses and the least extent of brain injury in the ME and LE groups, respectively. The mortality rate was positively correlated with the inoculum dose and the extent of inflammatory responses and brain injury. As blood culture was negative throughout the experiment, the inoculum dose-dependent increase in mortality, inflammatory responses, and brain injury solely reflects the virulence of EC5ME ventriculitis, without the confounding effects of the concomitant systemic bacteremia. Overall, these findings suggest that ME (5×10^2 CFU) of *E.coli* might be optimal inoculum dose to induce neonatal ventriculitis.

Because of the limitation stemming from the small sample size, the survival rate of the LE and ME groups may not be significantly different to that of NC group. Thus, for the next step, a large group experiment would be required. Furthermore, because of the small size of the rat pups, the CSF obtained with a cisternal tap was very small. It has been used primarily for bacterial culture but not enough CSF is obtained for measuring cytokines. We thus measured cytokine levels in brain tissue homogenates in this study. Using this model, to assess the long-term developmental delays including learning disability, memory deficit, or hearing abnormality, long-term follow-up study would be needed as a next step.

In infants with bacterial meningitis, brain MRI showed abnormalities including cerebral infarct, subdural empyema, cerebritis, and hydrocephalus.[19] Increased brain ventriculomegaly in the acute phase of bacterial meningitis in adults was associated with increased mortality.[29] In agreement with the clinical findings,[19,29] an acute inoculum dose-dependent increase in ventriculomegaly and cerebral infarct was observed at 1 day after the induction of ventriculitis. In addition, although a less absolute extent of ventriculomegaly and a higher extent of cerebral infarct were observed compared with post-inoculation day 1, the inoculum dose-dependent abnormalities persisted at 6 days after the induction of ventriculitis. Taken together, these findings suggested that brain MRI could be an early prognostic indicator that would be useful in identifying patients requiring further therapeutic interventions, and to assess the therapeutic efficacy of any new treatments, both in clinical and experimental settings of meningitis.[19,29]

Brain injuries observed in experimental models of neonatal meningitis are unique in consistently reproducing both hippocampal damage and cortical necrosis.[7–9] Inflammatory responses are primarily responsible for the ensuing brain injury in bacterial meningitis.[3,7,8,16] In the present study, the extent of inflammatory responses, both at post-inoculation day 1 and 6, and the increased number of TUNEL, GFAP, and ED-1-positive cells in the hippocampus at 1 day after induction of ventriculitis, were associated with the bacterial inoculum dose. Antibiotic treatment was started 24 h after bacterial inoculation and continued for 3 days; no bacteria were isolated, even in the CSF, at 5 days after the induction of ventriculitis. These findings suggest that increased inflammatory responses, but not increased bacterial proliferation and dissemination, triggered by a higher bacterial inoculum, are primarily responsible for the ensuing brain injury.

In summary, we successfully developed a newborn rat model of neonatal bacterial ventriculitis, without concomitant systemic bacteremia, by intraventricular injection of K1 capsule-negative *E. coli* at P11. We also determined that a bacterial inoculum dose of 5×10^2 CFU of EC5ME had the minimum mortality, and maximal inflammatory responses and ensuing brain injury. This animal model could provide the basis for both pathophysiology and intervention studies for neonatal bacterial ventriculitis not confounded by simultaneous systemic bacteremia. Hopefully, our newly developed newborn rat model of neonatal ventriculitis will lead to more detailed knowledge of, and new treatments for, this intractable and devastating disorder.

Acknowledgment

This work was supported by grant from the Korea Health Technology R&D Project through the Korea Health Industry Development Institute (KHIDI), funded by the Ministry of Health & Welfare, Republic of Korea (HI14C3484) and the Basic Science Research Program through the National Research Foundation of Korea (NRF) funded by the Ministry of Education, Science and Technology (NRF-2017R1D1A1B03035528, NRF-2017R1A2B2011383).

Disclosure

The authors declare no conflicts of interest.

Author contributions

Y.C. and S.A. contributed equally as co-first authors in conceptualizing the study design and hypothesis, data collection and analysis, manuscript writing and revision. W.P. contributed the study idea, design, and hypothesis, data collection and analysis, critically reviewed and revised the manuscript. D.S. and Y.K. contributed conceptualization of the study design, biochemical analysis and wrote a portion of the manuscript, and critically reviewed and revised the manuscript. All authors read and approved the final manuscript.

References

1 Anderson SG, Gilbert GL. Neonatal gram negative meningitis: a 10-year review, with reference to outcome and relapse of infection. *J. Paediatr. Child Health* 1990; **26**: 212–6.
2 Edwards MS, Rench MA, Haffar AA, Murphy MA, Desmond MM, Baker CJ. Long-term sequelae of group B streptococcal meningitis in infants. *J. Pediatr.* 1985; **106**: 717–22.
3 Polin RA, Harris MC. Neonatal bacterial meningitis. *Semin. Neonatol.* 2001; **6**: 157–72.
4 Park WS, Chang YS, Lee M. Effect of induced hyperglycemia on brain cell membrane function and energy metabolism during the early phase of experimental meningitis in newborn piglets. *Brain Res.* 1998; **798**: 195–203.
5 Tsao N, Chang WW, Liu CC, Lei HY. Development of hematogenous pneumococcal meningitis in adult mice: the role of TNF-alpha. *FEMS Immunol. Med. Microbiol.* 2002; **32**: 133–40.
6 Zwijnenburg PJ, van der Poll T, Florquin S, van Deventer SJ, Roord JJ, van Furth AM. Experimental pneumococcal meningitis in mice: a model of intranasal infection. *J. Infect. Dis.* 2001; **183**: 1143–6.
7 Grandgirard D, Steiner O, Tauber MG, Leib SL. An infant mouse model of brain damage in pneumococcal meningitis. *Acta Neuropathol.* 2007; **114**: 609–17.
8 Gianinazzi C, Grandgirard D, Imboden H *et al*. Caspase-3 mediates hippocampal apoptosis in pneumococcal meningitis. *Acta Neuropathol.* 2003; **105**: 499–507.
9 Brandt CT, Holm D, Liptrot M *et al*. Impact of bacteremia on the pathogenesis of experimental pneumococcal meningitis. *J. Infect. Dis.* 2008; **197**: 235–44.
10 Tauber MG, Sande MA. Pathogenesis of bacterial meningitis: contributions by experimental models in rabbits. *Infection* 1984; **12** (Suppl 1): S3–10.
11 Chiavolini D, Pozzi G, Ricci S. Animal models of Streptococcus pneumoniae disease. *Clin. Microbiol. Rev.* 2008; **21**: 666–85.
12 Kim KS, Itabashi H, Gemski P, Sadoff J, Warren RL, Cross AS. The K1 capsule is the critical determinant in the development of *Escherichia coli* meningitis in the rat. *J. Clin. Investig.* 1992; **90**: 897–905.
13 Holler JG, Brandt CT, Leib SL, Rowland IJ, Ostergaard C. Increase in hippocampal water diffusion and volume during

experimental pneumococcal meningitis is aggravated by bacteremia. *BMC Infect. Dis.* 2014; **14**: 240.
14 Ostergaard C, Leib SL, Rowland I, Brandt CT. Bacteremia causes hippocampal apoptosis in experimental pneumococcal meningitis. *BMC Infect. Dis.* 2010; **10**: 1.
15 Brandt CT, Lundgren JD, Frimodt-Moller N *et al*. Blocking of leukocyte accumulation in the cerebrospinal fluid augments bacteremia and increases lethality in experimental pneumococcal meningitis. *J. Neuroimmunol.* 2005; **166**: 126–31.
16 Kim KS. Pathogenesis of bacterial meningitis: from bacteraemia to neuronal injury. *Nat. Rev. Neurosci.* 2003; **4**: 376–85.
17 Chua C. Neonatal meningitis and ventriculitis. *J. Natl Med. Assoc.* 1978; **70**: 794–5.
18 Berman PH, Banker BQ. Neonatal meningitis. A clinical and pathological study of 29 cases. *Pediatrics* 1966; **38**: 6–24.
19 Brandt CT, Simonsen H, Liptrot M *et al*. In vivo study of experimental pneumococcal meningitis using magnetic resonance imaging. *BMC Med. Imaging* 2008; **8**: 1.
20 Ahn SY, Chang YS, Sung DK *et al*. Mesenchymal stem cells prevent hydrocephalus after severe intraventricular hemorrhage. *Stroke* 2013; **44**: 497–504.
21 Ahn SY, Chang YS, Sung DK, Sung SI, Ahn JY, Park WS. Pivotal Role of brain-derived neurotrophic factor secreted by mesenchymal stem cells in severe intraventricular hemorrhage in newborn rats. *Cell Transplant.* 2017; **26**: 145–56.
22 Ahn SY, Chang YS, Sung DK *et al*. Optimal route for mesenchymal stem cells transplantation after severe intraventricular hemorrhage in newborn rats. *PLoS ONE* 2015; **10**: e0132919.
23 Romijn HJ, Hofman MA, Gramsbergen A. At what age is the developing cerebral cortex of the rat comparable to that of the full-term newborn human baby? *Early Human Dev.* 1991; **26**: 61–7.
24 Kim ES, Ahn SY, Im GH *et al*. Human umbilical cord blood-derived mesenchymal stem cell transplantation attenuates severe brain injury by permanent middle cerebral artery occlusion in newborn rats. *Pediatr. Res.* 2012; **72**: 277–84.
25 Park WS, Sung SI, Ahn SY *et al*. Hypothermia augments neuroprotective activity of mesenchymal stem cells for neonatal hypoxic-ischemic encephalopathy. *PLoS ONE* 2015; **10**: e0120893.
26 Daum RS, Scheifele DW, Syriopoulou VP, Averill D, Smith AL. Ventricular involvement in experimental Hemophilus influenzae meningitis. *J. Pediatr.* 1978; **93**: 927–30.
27 Gilles FH, Jammes JL. Berenberg W. Neonatal meningitis. The ventricle as a bacterial reservoir. *Arch. Neurol.* 1977; **34**: 560–2.
28 Friede RL. Cerebral infarcts complicating neonatal leptomeningitis. *Acta Neuropathol.* 1973; **23**: 245–53.
29 Sporrborn JL, Knudsen GB, Solling M *et al*. Brain ventricular dimensions and relationship to outcome in adult patients with bacterial meningitis. *BMC Infect. Dis.* 2015; **15**: 367.

Supporting Information

Additional Supporting Information may be found in the online version of this article at the publisher's web-site:

Appendix S1. Representative photomicrographs of TUNEL and GFAP (glial fibrillary acidic protein) stained brain histologic section in P17 rats those received needle injection procedure only without any treatment.